

## Atmospheric Hydrogen Cyanide (HCN): Biomass Burning Source, Ocean Sink?

Qinbin Li, Daniel J. Jacob, Isabelle Bey, Robert M. Yantosca

Department of Earth and Planetary Sciences and Division of Engineering and Applied Sciences, Harvard University, Cambridge, Massachusetts

Yongjing Zhao,<sup>1</sup> Yutaka Kondo

Solar-Terrestrial Environment Laboratory, Nagoya University, Toyokawa, Japan

Justus Notholt

Alfred Wegener Institute for Polar and Marine Research, Potsdam, Germany

**Abstract.** The observed seasonal amplitude of atmospheric HCN concentrations implies an atmospheric lifetime of only a few months for HCN, much shorter than is commonly assumed from oxidation by OH (a few years). We propose that ocean uptake provides the missing sink, and show with a global 3-D model simulation that the observations of atmospheric HCN can be roughly reproduced in a scenario where biomass burning provides the main source (1.4–2.9 Tg N yr<sup>-1</sup>) and ocean uptake provides the main sink (HCN atmospheric lifetime of 2–4 months). Such a budget implies that HCN is a sensitive tracer of biomass burning on large scales, of particular value because it is readily observed from space. The ocean sink hypothesis can be tested with measurements of HCN concentrations in marine air and seawater.

### Introduction

Spectroscopic measurements of the atmospheric column of HCN at northern midlatitudes indicate factors of 2–3 seasonal variation with maxima in spring-summer [Mahieu *et al.*, 1995, 1997; Zhao *et al.*, 1999]. Space-based measurements of HCN mixing ratios in the tropical upper troposphere indicate a range from 200 to 900 pptv [Rinsland *et al.*, 1998]. Such large variations are inconsistent with the conventional view that HCN has an atmospheric lifetime of a few years with oxidation by OH providing the main sink [Cicerone and Zellner, 1983]. There must be a large missing sink of HCN imposing a lifetime of a few months. Improved understanding is needed because HCN (1) interferes with measurements of total reactive nitrogen (NO<sub>y</sub>) [Kondo

*et al.*, 1997], (2) could play a non-negligible role in the biogeochemical cycling of nitrogen, and (3) provides a tracer of biomass burning readily observable from space [Rinsland *et al.*, 1998].

We propose here that ocean uptake could provide the missing sink for atmospheric HCN, and show with a global 3-D model that the available observations of atmospheric HCN are consistent with a scenario where biomass burning provides the main source and ocean uptake provides the main sink. The Henry's law constant of HCN is sufficiently high (12 M atm<sup>-1</sup> at 298 K; Edwards *et al.*, [1978]) for ocean uptake to impose an atmospheric lifetime of a few months if HCN(aq)/CN<sup>-</sup> (*pKa* = 9.2) is consumed chemically or biologically in the ocean on a time scale of a few months or less, as discussed below. There are to our knowledge no data on HCN(aq)/CN<sup>-</sup> concentrations in the oceans.

It is well established that biomass burning is a major source of atmospheric HCN, though different studies indicate a range of molar emission ratios relative to CO (0.03–1.1%) [Lobert *et al.*, 1990; Hurst *et al.*, 1994; Yokelson *et al.*, 1997; Holzinger *et al.*, 1999]. Lobert *et al.* [1990] estimate a global source of HCN from biomass burning of 0.4–1.9 Tg N yr<sup>-1</sup>. Lobert [1989] estimates a global fossil fuel combustion source of 0.04 Tg N yr<sup>-1</sup>, negligibly small in comparison. Higher plants and fungi are known to produce and release HCN, but the available data do not allow a quantitative estimate of emissions [Cicerone and Zellner, 1983]. A possible HCN source in the stratosphere is ion-catalyzed conversion of CH<sub>3</sub>CN [Schneider *et al.*, 1997].

### Model Simulation

We use the Harvard-GEOS global 3-D model to simulate atmospheric HCN. The model is driven by 1993–1994 meteorological data updated every 6 hours from the Goddard Earth Observing System Data Assimilation System (GEOS-1 DAS) [Schubert *et al.*, 1993]. Advection is computed following Lin and Rood [1996]. Moist convection and boundary layer mixing are com-

<sup>1</sup>Now at Department of Physics, University of Toronto, Toronto, Canada.

puted following *Allen et al.* [1996]. The spatial resolution is  $4^\circ$  latitude by  $5^\circ$  longitude, with twenty  $\sigma$  vertical levels up to 10 hPa. We use a zero-flux boundary condition at 10 hPa. A six-year simulation is conducted, recycling the meteorological fields for 1993–1994, to remove the effect of the initial condition (170 pptv HCN). Previous tracer model studies indicate that the GEOS fields provide a reasonable simulation of global atmospheric transport [*Allen et al.*, 1996; *Bey et al.*, 1999].

We adopt in our standard simulation an HCN biomass burning emission ratio of 1.1% relative to CO on a molar basis, which is at the high end of laboratory data but is most consistent with observed HCN-CO column correlations [*Rinsland et al.*, 1998, 1999]. We could accommodate a smaller emission ratio depending on the efficacy of the ocean sink, as will be discussed later. We combine the HCN emission ratio with the biomass burning CO emission inventory of *Wang et al.* [1998]. This inventory has  $1^\circ \times 1^\circ$  spatial resolution and monthly temporal resolution. The resulting global biomass burning source of HCN is  $2.9 \text{ Tg N yr}^{-1}$ . There are no other HCN sources in our model.

The ocean uptake flux of HCN is  $F = k_w C_g K_H RT$

**Table 1.** Atmospheric Budget of HCN

Total atmospheric burden (Tg N)	0.50
Atmospheric lifetime	2.1–4.4 months
Sources (Tg N yr <sup>-1</sup> ):	
Biomass burning	1.4–2.9
Sinks (Tg N yr <sup>-1</sup> ):	
Ocean uptake	1.1–2.6
Reaction with OH	0.3
Photolysis	$0.2 \times 10^{-2}$
Reaction with O( <sup>1</sup> D)	$0.3 \times 10^{-3}$

Global budget for 1000–10 hPa.

[*Liss and Slater*, 1974], where  $k_w$  ( $\text{m s}^{-1}$ ) is the air-to-sea transfer velocity,  $C_g$  ( $\text{kg m}^{-3}$ ) is the concentration of HCN in surface air,  $R$  is the gas constant,  $T$  is temperature, and  $K_H$  is the temperature-dependent Henry's law constant with  $K_H = 12 \text{ M atm}^{-1}$  at 298 K and  $\Delta H_{298}/R = -5000 \text{ K}$  [*Edwards et al.*, 1978]. Diffusion in the liquid phase controls the oceanic uptake of HCN. We adopt  $k_w = 0.31 u^2 (Sc/660)^{-1/2}$  with  $u$  in  $\text{m s}^{-1}$  and  $k_w$  in  $\text{cm hr}^{-1}$  [*Wanninkhof*, 1992], where  $u$  is the wind speed at 10 m height,  $Sc = \nu/D$  is the Schmidt

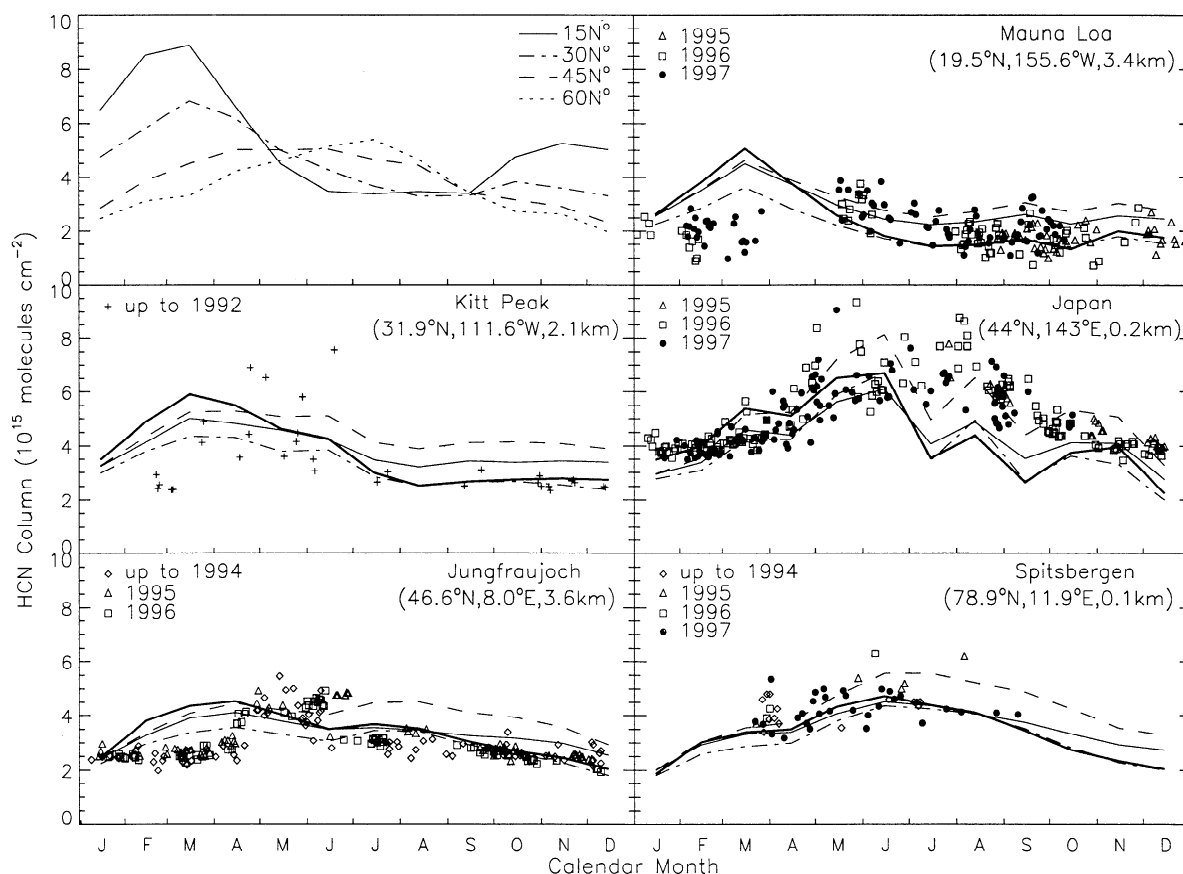


**Figure 1.** Seasonal variation of HCN column concentrations. Individual observations are shown as symbols. Monthly mean model values are shown as lines for the standard simulation (thick solid lines) and for three sensitivity simulations: 1) ocean uptake and biomass burning source reduced by factors of 6 and 2, respectively (thin solid lines); 2) ocean uptake and tropical HCN emission ratio reduced by factors of 6 and 2, respectively (dashed lines); 3) both ocean uptake and tropical HCN emission ratio reduced by a factor of 2 (dash-dot lines). The top left panel shows zonally averaged model values in the standard simulation for different latitudes of the northern hemisphere.

number of HCN in seawater,  $\nu$  is the kinematic viscosity of water, and  $D$  is the diffusion coefficient of HCN in water. We assume that there is no reverse sea-to-air transfer flux, i.e., that  $\text{HCN}(\text{aq})/\text{CN}^-$  is consumed in the oceans. A sensitivity simulation where  $k_w$  is reduced by a factor of 6 (to describe a situation where 5/6 of the HCN taken up by the oceans is returned to the atmosphere, i.e., a saturation ratio of 0.83) is still capable of reproducing the observed seasonal variations as discussed below. This sensitivity simulation corresponds to an  $\text{HCN}(\text{aq})/\text{CN}^-$  lifetime of 2–3 months against consumption in the oceanic mixed layer.

Additional sinks for atmospheric HCN from photolysis and reactions with OH and  $\text{O}(^1D)$  are specified following Cicerone and Zellner [1983]. Monthly varying concentration fields of tropospheric OH are taken from Bey *et al.* [1999], and monthly varying concentration fields of stratospheric OH and  $\text{O}(^1D)$  are taken from Schneider *et al.* [1999].

Our global budget of atmospheric HCN is shown in Table 1. The range is bounded by the standard simulation and by a sensitivity simulation where HCN emission is reduced by 53% and where 5/6 of HCN taken up by the ocean is returned to the atmosphere, resulting in the same atmospheric inventory of HCN as in the standard case (see Figure 1 and discussion below). The atmospheric lifetime of HCN is 2.1–4.4 months, with ocean uptake providing the main sink. The HCN ocean uptake of 1.1–2.6 Tg N yr<sup>-1</sup> can be compared to an estimated 30 Tg N yr<sup>-1</sup> total input of atmospheric fixed N to the oceans [Duce *et al.*, 1991]. Long-range transport of HCN could make a significant contribution to the deposition flux of fixed N to the central regions of the oceans.

## Results and Discussion

Figure 1 compares model results to observed HCN columns at Jungfraujoch in the Swiss Alps [Mahieu *et al.*, 1995, 1997], Kitt Peak in Arizona [Mahieu *et al.*, 1995], Mauna Loa in Hawaii [Rinsland *et al.*, 1999], Rikubetsu and Moshiri in Japan [Zhao *et al.*, 1999], and Ny Ålesund in Spitsbergen (J. Notholt, unpublished data, 1999). Observations after September 1997 are not included in Figure 1 because of anomalous enhancements from massive fires in Indonesia [Rinsland *et al.*, 1999] which we will examine in a separate study.

The observations in Figure 1 were made by measuring absorption of solar radiation in the 3299.53 cm<sup>-1</sup> and 3287.25 cm<sup>-1</sup> HCN absorption bands; HCN columns were retrieved by assuming a vertical profile of HCN mixing ratios, typically uniform in the troposphere and decreasing with altitude in the stratosphere. In our model the tropospheric mixing ratio of HCN increases with altitude outside of source regions because of the ocean sink. We did not attempt to resolve inconsistencies between the model vertical profiles of mixing ratios and the assumed profiles used in the retrievals of the observed columns.

The observations show factors of  $\sim 2$  seasonal amplitude with maxima in April–August. The model reproduces roughly the observed seasonal amplitudes but precedes the observed maxima by 1–2 months. As shown in the first panel of Figure 1, the model maxima reflect the northward propagation of the signal from biomass burning in the northern tropics which peaks in February, combined with the smaller signal from boreal forest fires which peaks in the summer.

The phase precession in the model compared to observations suggests either a flaw in the prescribed seasonal pattern of biomass burning emissions or a major HCN source other than biomass burning. Mahieu *et al.* [1995] attributed the spring maxima at Jungfraujoch and Kitt Peak to a biogenic source. However, the strong correlation observed between HCN and CO columns at Jungfraujoch (E. Mahieu, personal communication, 1999), at the Japanese sites [Zhao *et al.*, 1999] and at Mauna Loa [Rinsland *et al.*, 1999], supports a dominant biomass burning source. Ship measurements of atmospheric HCN columns over the tropical Atlantic in October [Notholt *et al.*, 1999] indicate elevated values associated with elevated CO and clearly associated with biomass burning. Our model values over the tropical Atlantic are twice those observed by Notholt *et al.* [1999], suggesting that our HCN tropical emission ratio is too high. Since HCN is a product of smoldering rather than flaming combustion [Lobert *et al.*, 1990], one would expect lower emission ratios from tropical savanna fires than from midlatitude forest fires. A sensitivity model simulation with tropical HCN emission ratios and ocean uptake both reduced by a factor of 2 (Figure 1) yields results over the tropical Atlantic that agree fairly well with the Notholt *et al.* [1999] observations (not shown).

Figure 2 presents simulated zonal mean, yearly averaged mixing ratios of HCN. Simulated mixing ratios are minimum in the marine boundary layer (10–100 pptv) and maximum over biomass burning regions (up to 2000

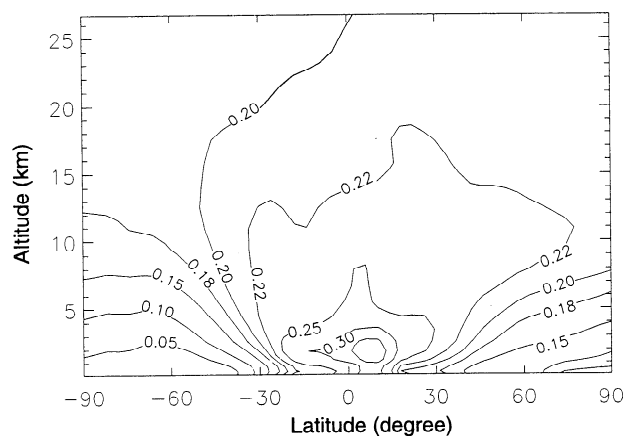


**Figure 2.** Annual mean, zonally averaged mixing ratios of HCN in the standard simulation. Contour levels (ppbv) are 0.05, 0.1, 0.15, 0.18, 0.2, 0.22, 0.25, 0.3, and 0.35.

pptv in the boundary layer and 500 pptv in the upper troposphere, consistent with the observations of Rinsland *et al.* [1998]). There are to our knowledge no measurements of HCN mixing ratios in the marine boundary layer (or, in fact, anywhere in the lower troposphere). Measurements in the stratosphere show HCN mixing ratios in the range 170–200 pptv [Spreng and Arnold, 1994]. The model simulates 180–220 pptv in the stratosphere; the stratospheric sink of HCN may be underestimated because of the zero-flux boundary condition at 10 hPa.

We have assumed in the standard simulation a relatively high air-to-sea transfer velocity [Wanninkhof, 1992] and neglected any reverse sea-to-air transfer. Our results are only moderately sensitive to these assumptions because the ocean uptake is largely limited by vertical transport from the free troposphere to the marine boundary layer. We could accommodate a decrease in the ocean sink by decreasing the biomass burning source down to a point limited by the ability of the model to reproduce the relative seasonal amplitude in the observations. As shown in Figure 1, a sensitivity simulation with the net ocean uptake reduced by a factor of 6 (see previous section) still provides a fair comparison to observations. This simulation corresponds to an atmospheric lifetime of HCN of 4.4 months and a 53% reduction in the biomass burning source ( $1.4 \text{ Tg N yr}^{-1}$ ) to achieve the same atmospheric inventory of HCN as in the standard simulation.

**Acknowledgments.** This work was funded by the National Science Foundation and by the National Aeronautics and Space Administration. Discussions with B. Heikes, J. Logan, M. Schultz, and O. Zafriou were very helpful.

## References

- Allen, D. J., R. B. Rood, A. M. Thompson, and R. D. Hudson, Three dimensional radon 222 simulations using assimilated meteorological data and a convective mixing algorithm, *J. Geophys. Res.*, **101**, 6871–6882, 1996.
- Bey, I., R. M. Yantosca, and D. J. Jacob, Export of pollutants from eastern Asia: A simulation of the PEM-West (B) aircraft mission using a 3-D model driven by assimilated meteorological fields, *EOS Trans. AGU*, **80**, (17), S31, 1999.
- Cicerone, R. J., and R. Zellner, The atmospheric chemistry of hydrogen cyanide (HCN), *J. Geophys. Res.*, **88**, 10,689–10,696, 1983.
- Duce, R. A. *et al.*, The atmospheric input of trace species to the world ocean, *Global Biogeochemical Cycles*, **5**, 193–259, 1991.
- Edwards, T. J., G. Maurer, J. Newman, and J. M. Prausnitz, Vapor-liquid equilibria in multicomponent aqueous solutions of volatile weak electrolytes, *AIChE J.*, **24**, 966–976, 1978.
- Holzinger, R. *et al.*, Biomass burning as a source of formaldehyde, acetaldehyde, methanol, acetone, acetonitrile, and hydrogen cyanide, *Geophys. Res. Lett.*, **26**, 1161–1164, 1999.
- Hurst, D. F., D. W. T. Griffith, and G. D. Cook, Trace gas emissions from biomass burning in tropical Australian savannas, *J. Geophys. Res.*, **99**, 16,441–16,456, 1994.
- Kondo, Y. *et al.*, The performance of an aircraft instrument for the measurement of  $\text{NO}_y$ , *J. Geophys. Res.*, **102**, 28,663–28,671, 1997.
- Lin, S.-J., and R. B. Rood, Multidimensional flux form semi-Lagrangian transport schemes, *Mon. Weather Rev.*, **124**, 2046–2070, 1996.
- Liss, P. S., and P. G. Slater, Flux of gases across the air-sea interface, *Nature*, **247**, 181–184, 1974.
- Lobert, J. M., Verbrennungen pflanzlicher biomasse als Quelle atmosphärischer Spurengase: Cyanoverbindungen,  $\text{CO}$ ,  $\text{CO}_2$ , und  $\text{NO}_x$ . Ph.D. thesis, Johannes Gutenberg Universität, Mainz, 1989.
- Lobert, J. M., D. H. Scharffe, W. M. Hao, and P. J. Crutzen, Importance of biomass burning in the atmospheric budgets of nitrogen-containing gases, *Nature*, **346**, 552–554, 1990.
- Mahieu, E., C. P. Rinsland, R. Zander, P. Demoulin, L. Delbouille, and G. Roland, Vertical column abundances of HCN deduced from ground-based infrared solar spectra: Long-term trend and variability, *J. Atmos. Chem.*, **20**, 299–310, 1995.
- Mahieu, E., R. Zander, L. Delbouille, P. Demoulin, G. Roland, and C. Servais, Observed trends in total vertical column abundances of atmospheric gases from IR solar spectra recorded at the Jungfraujoch, *J. Atmos. Chem.*, **28**, 227–243, 1997.
- Notholt, J. *et al.*, Latitudinal variations of trace gas concentrations in the free troposphere measured by solar absorption spectroscopy during a ship cruise, *J. Geophys. Res.*, in press, 1999.
- Rinsland, C. P. *et al.*, ATMOS/ATLAS 3 infrared profile measurements of trace gases in the November 1994 tropical and subtropical upper troposphere, *J. Quant. Spectrosc. Radiat. Transfer*, **60**, 891–901, 1998.
- Rinsland, C. P. *et al.*, Infrared solar spectroscopic measurements of free tropospheric  $\text{CO}$ ,  $\text{C}_2\text{H}_6$ , and HCN above Mauna Loa, Hawaii: Seasonal variations and evidence for enhanced emissions from the southeast Asian tropical fires of 1997–1998, *J. Geophys. Res.*, **104**, 18,667–18,680, 1999.
- Schneider, H. R., D. B. A. Jones, G.-Y. Shi, and M. B. McElroy, Analysis of residual mean transport in the stratosphere. Part 1: Model description and comparison with satellite data, *J. Geophys. Res.*, in press, 1999.
- Schneider, J., V. Bürger, and F. Arnold, Methyl cyanide and hydrogen cyanide measurements in the lower stratosphere: Implications for methyl cyanide sources and sinks, *J. Geophys. Res.*, **102**, 25,501–25,506, 1997.
- Schubert, S. D., R. B. Rood, and J. Pfandner, An assimilated data set for Earth Science applications, *Bull. Am. Meteorol. Soc.*, **74**, 2331–2342, 1993.
- Spreng, S., and F. Arnold, Balloon-borne mass spectrometer measurements of  $\text{HNO}_3$  and HCN in the winter Arctic stratosphere—Evidence for  $\text{HNO}_2$ -processing by aerosols, *Geophys. Res. Lett.*, **21**, 1251–1254, 1994.
- Wang, Y., D. J. Jacob, and J. A. Logan, Global simulation of tropospheric  $\text{O}_x$ - $\text{NO}_x$ -hydrocarbon chemistry, 1. Model formulation, *J. Geophys. Res.*, **103**, 10,713–10,725, 1998.
- Wanninkhof, R., Relationship between wind speed and gas exchange over the ocean, *J. Geophys. Res.*, **97**, 7373–7382, 1992.
- Yokelson, R. J., R. Susott, D. E. Ward, J. Reardon, and D. W. T. Griffith, Emissions from smoldering combustion of biomass measured by open-path Fourier transform infrared spectroscopy, *J. Geophys. Res.*, **102**, 18,865–18,877, 1997.
- Zhao, Y. *et al.*, Seasonal variations of HCN over northern Japan measured by ground-based infrared solar spectroscopy, submitted to *Geophys. Res. Lett.*, 1999.

(Received July 19, 1999; revised November 26, 1999; accepted December 7, 1999.)